ELECTRONIC SUPPLEMENTARY INFORMATION

Nanoconfinement Effects on Structural Anomalies in Imidazolium Ionic Liquids

Mikhail Yu. Ivanov,[†,‡,*] Artem S. Poryvaev,[†,‡,II] Daniil M. Polyukhov,[†] Sergey A. Prikhod'ko,[§] Nicolay Yu. Adonin,[§] Matvey V. Fedin [†,‡,*]

[†]*International Tomography Center SB RAS, Institutskaya Street 3a, 630090 Novosibirsk, Russia*
[‡]*Novosibirsk State University, Pirogova Street 2, 630090 Novosibirsk, Russia*
[§]*Boreskov Institute of Catalysis SB RAS, Lavrentiev Avenue 5, 630090 Novosibirsk, Russia*
[II]*N. N. Vorozhtsov Novosibirsk Institute of Organic Chemistry SB RAS, Lavrentiev Avenue 9, 630090 Novosibirsk, Russia*

email: michael.ivanov@tomo.nsc.ru, mfedin@tomo.nsc.ru

Table of Contents

I. Experimental section

Ionic liquids [Bmim]Cl, [Bmim]BF_4, [Bmim]PF_6 and [Bmim]CF_3SO_3 were synthesized according to the procedures described in Ref.S2. The purity of the obtained compounds was verified using NMR.

The spiro-cyclohexane-substituted nitroxide N1 (14-carbamoyl-7-azadispiro[5.1.5.2]pentadeca-14-ene-7-oxyl) was prepared according to literature protocol.[S2] TEMPO-D_{18} radical ((2,2,6,6-tetramethylpiperidin-1-yl)oxyl) was used as mentioned in the previous study.[S3] The final concentration of spin probe in IL was about 1 mM.

For the series of "N1+[Bmim]X" samples, nitroxide was dissolved in the corresponding IL in concentrations of ~1 mM. Next, the solution was placed in the EPR quartz tube (inner diameter of 2.8 mm), evacuated at 10^{-5} mbar with simultaneous heating at 85 °C for 12 hours to reduce the amount of remaining water and to eliminate the remaining oxygen, exposed to 3–5 freeze–pump–thaw cycles, and finally sealed off under vacuum.

For the series of "N1@ZIF-8 + [Bmim]X" samples, the following procedure for IL impregnation was used. Around 10mg of N1@ZIF-8 powder sample were placed into EPR quartz tube (inner diameter of 2.8 mm). Then 100 µL of corresponding ionic liquid were added into the quartz tube with powder. The obtained samples were evacuated at 10^{-5} mbar with simultaneous heating at 90^{o}C during 12 hours. Then quartz tubes with samples were sealed off by flame.

Pulse EPR measurements were performed using a commercial Bruker Elexsys E580 spectrometer at X-band. The spectrometer was equipped with an Oxford Instruments temperature control system (4−300 K). The echo-detected EPR spectra and transverse relaxation (phase memory) times T_2 were recorded using the standard two-pulse Hahn echo sequence π/2−τ−π−τ−echo with pulse lengths 100/50 ns for π and π/2 pulses. Monoexponential analysis of echo decay vs. 2τ yields the corresponding T_2 value at certain magnetic field. CW EPR spectra were acquired using an X-band Bruker EMX spectrometer (9 GHz). In all experiments the sample was first shock-frozen in liquid nitrogen and then transferred into the cryostat. In this way we ensured that the sample was in glassy state at the beginning of each experiment. The heating/cooling rates were ca. 1 K/min; the sample was equilibrated for at least 10 minutes prior to each EPR measurement. All spectral simulations were done using EasySpin.[S4]

II. Synthesis of ionic liquids

BmimCl were obtained by analogy with the literature method[S1] from 1-methyl imidazole and butyl chloride.

Diffrernt anion-containing ionic liquids
A 100 ml round-bottomed flask fitted with magnetic stirrer bar and reflux condenser was charged by 4.63 g (26.5 mmol) BmimCl, 53 mmol of corresponding salt ($NaBF_4$, $NaPF_6$, CF_3SO_3Na) and 80 ml of acetone. The mixture was stirred for 3 hours at 50 °C. The solid was filtered and washed by 10 ml of acetone. The second portion of corresponding salt (20 mmol) was added to the filtrate and the resulting mixture was stirred for 3 hours at 50 °C. The solid was filtered and washed by 10 ml of acetone. The filtrate was evaporated in vacuum. The residue was solved in 30 ml of dry dichloromethane (to remove NaCl and excess of starting salt) and filtered. The filtrate was evaporated and product was dried in high vacuum (10^{-3} bar) at 80 °C for 6 hours. Yield of products are 75-85 %. The reaction of sample of ionic liquid with $AgNO_3$ was negative, that demonstrates the absence of Cl^- ions in the ionic liquid media.

The NMR spectral data of ionic liquids
The NMR spectra were recorded on a Bruker AVANCE 300 spectrometer (^1H at 300.13 MHz, ^{19}F at 282.40 MHz). The chemical shifts are referenced to TMS (^1H), CCl_3F (^{19}F, with C_6F_6 as secondary reference (-162.9 ppm))

1-Butyl-3-methylimidazolium tetrafluoroborate ([Bmim]BF_4)
^{1}H NMR ($CDCl_3$): δ 8.83 (s, 1H, *H*-2); 7.31 (s, 1H, *H*-4); 7.26 (s, 1H, *H*-5); 4.16 (t, 2H, $^3J_{HH}$ 7.4 Hz, α-C*H*$_2$); 3.94 (s, 3H, NC*H*$_3$); 1.84 (tt, 2H, $^3J_{HH}$ 7.4 Hz, $^3J_{HH}$ 7.4 Hz, β-C*H*$_2$); 1.35 (qt, 2H, $^3J_{HH}$ 7.4 Hz, $^3J_{HH}$ 7.5 Hz, γ-C*H*$_2$); 0.84 (t, 3H, $^3J_{HH}$ 7.4 Hz, δ-C*H*$_3$).
^{19}F NMR ($CDCl_3$): δ -152.67 (s, 4F, B*F*$_4$).

1-Butyl-3-methylimidazolium hexafluorophosphate ([Bmim]PF_6)
^{1}H NMR ($CDCl_3$): δ 8.98 (s, 1H, *H*-2); 7.72 (s, 2H, *H*-4, *H*-5); 4.15 (t, 2H, $^3J_{HH}$ 7.4 Hz, α-C*H*$_2$); 3.85 (s, 3H, NC*H*$_3$); 1.77 (tt, 2H, $^3J_{HH}$ 7.5 Hz, $^3J_{HH}$ 7.5 Hz, β-C*H*$_2$); 1.30 (qt, 2H, $^3J_{HH}$ 7.5 Hz, $^3J_{HH}$ 7.5 Hz, γ-C*H*$_2$); 0.93 (t, 3H, $^3J_{HH}$ 7.4 Hz, δ-C*H*$_3$).
^{19}F NMR ($CDCl_3$): δ -66.21, -68.09 (2s, 6F, *PF*$_6$).

1-Butyl-3-methylimidazolium trifluoromethyl sulphonate ([Bmim]CF_3SO_3)
^{1}H NMR ($CDCl_3$): δ 8.85 (s, 1H, *H*-2); 7.32 (s, 2H, *H*-4, *H*-5); 4.04 (t, 2H, $^3J_{HH}$ 7.4 Hz, α-C*H*$_2$); 3.81 (s, 3H, NC*H*$_3$); 1.70 (tt, 2H, $^3J_{HH}$ 7.5 Hz, $^3J_{HH}$ 7.5 Hz, β-C*H*$_2$); 1.19 (qt, 2H, $^3J_{HH}$ 7.5 Hz, $^3J_{HH}$ 7.5 Hz, γ-C*H*$_2$); 0.78 (t, 3H, $^3J_{HH}$ 7.4 Hz, δ-C*H*$_3$).
^{19}F NMR ($CDCl_3$): δ -80.26 (s, 3F, C*F*$_3$*SO*$_3$).

III. Synthesis of N1@ZIF-8 MOF

The synthesis was carried out according to a typical procedure for ZIF-8 water based synthesis[S5] with minor modifications. The modifications were necessary to incorporate stable radical N1 into the ZIF-8 cavities. 0.337g of anhydrous $ZnCl_2$ (2.5 mmol) were dissolved in 10 ml of deionized water and added to a solution of N1 with 2-methylimidazole (HMeIm). N1/HMeIm solution was prepared by dissolving 12.3 g of HMeIm (0.15 mol) in 90 ml of deionized water and adding 2 mg of N1 (0.007 mmol) to the solution. The final molar composition of the synthesis solution was Zn^{2+}: HMeIm : N1 : water = 1 : 60 : 0.003 : 2228. The mixture was stirred at room temperature during 6 days. Then N1@ZIF-8 suspension was centrifuged and washed three times with deionized water and five times with methanol. The product was first dried for 24h at room temperature, and then under reduced pressure at 333 K during next 24h.

To confirm ZIF-8 stability in IL we impregnated the powder of ZIF-8 by [Bmim]PF_6. This IL was selected because the EPR spectra of impregnated N1@ZIF-8 contained two fractions (see Fig.1 and Table 1), therefore additional validation was invited. The sample was heated at 100˚C for 12 hours, then shock-frozen at 77 K for 1 min, and then kept 3 days at room temperature. In this way we exposed sample to all possible stress factors during EPR experiments. Next, we separated the IL and the powder using centrifugal PTFE membrane (0.22 μm) and analyzed both fractions using EPR at room temperature. Radical content in solid N1@ZIF-8 fraction did not decrease after performed actions. Also, the radical signal in pure liquid IL fraction was not found. This experiment unambiguously confirms that ZIF-8 is not soluble in [Bmim]PF_6 (at least, in our experimental conditions), and that radical is not capable to escape from ZIF-8 confinement when MOF is impregnated by IL.

IV. Simulation parameters for CW EPR experiments

Table S1 lists the spectroscopic parameters used to simulate EPR spectra shown in Figure 1 of the main text. Two components of the line width correspond to [Gaussian Lorentzian].

Table S1. Simulation parameters for the CW EPR spectra shown in Figure 1.

sample	**$[g_{xx}\ g_{yy}\ g_{zz}]$**		**$[A_{xx}\ A_{yy}\ A_{zz}]$ / mT**	**τ_c / ns**	**Line width Γ / mT**
Bare N1@ZIF-8	[2.0115, 2.0086, 2.0035]		[0.48, 0.48, 3.35]	0.4	[0.00 1.60]
N1@ZIF-8+ [Bmim]BF_4	[2.0115, 2.0080, 2.0040]		[0.50, 0.50, 3.47]	25.1	[0.68 0.00]
N1@ZIF-8+ [Bmim]CF_3SO_3	[2.0115, 2.0080, 2.0040]		[0.50, 0.50, 3.60]	17.8	[0.60 0.00]
N1@ZIF-8+ [Bmim]Cl	[2.0115, 2.0080, 2.0040]		[0.50, 0.50, 3.47]	22.4	[0.75 0.00]
N1@ZIF-8+ [Bmim]Br	[2.0115, 2.0080, 2.0040]		[0.50, 0.50, 3.47]	22.4	[0.75 0.00]
N1@ZIF-8+ [Bmim]PF_6	50%	[2.0115, 2.0080, 2.0040]	[0.50, 0.50, 3.47]	25.1	[0.68 0.00]
	50%	[2.0115, 2.0085, 2.0045]	[0.52, 0.52, 3.60]	2.2	[0.50 0.00]
N1+[Bmim]PF_6	[2.0115, 2.0085, 2.0035]		[0.52, 0.52, 3.60]	3.5	[0.40 0.00]
N1+[Bmim]BF_4	[2.0115, 2.0085, 2.0035]		[0.52, 0.52, 3.45]	1.6	[0.55 0.00]
N1+[Bmim]CF_3SO_3	[2.0115, 2.0085, 2.0035]		[0.52, 0.52, 3.45]	2.0	[0.50 0.00]
N1+[Bmim]Cl	[2.0115, 2.0085, 2.0035]		[0.45, 0.45, 3.40]	8.9	[0.55 0.00]
N1+[Bmim]Br	[2.0115, 2.0080, 2.0035]		[0.48, 0.48, 3.45]	15.8	[0.60 0.00]

V. EPR of stochastic molecular librations (brief tutorial)

In order to introduce interested reader to the approach of EPR-detected stochastic molecular librations, we present this purely educational section. More specific information can be found in the provided references.

EPR is a very useful tool to investigate the mobility of paramagnetic molecules in various media. In particular, stochastic molecular librations of molecules commonly occur in molecular glasses. They represent the small-angle wobbling of molecules driven by thermal energy. When spin probe, most often the nitroxide radical, is placed in glass, it exhibits similar librations to those occurring in the surrounding matrix. In other words, being tightly embedded in the glass, the spin probe follows its molecular mobility/wobbling. This makes spin probes in the glasses true reporters of the state of the surrounding matrix.

EPR is generally sensitive to the mobility of the nitroxide probe. Most commonly, the shape of CW EPR spectrum allows one to determine the rotational correlation times of the nitroxide. However, when the mobility is restricted to small-angle wobbling (e.g. $<1^{o}$), CW EPR becomes insensitive. At the same time, pulse EPR based relaxation methods come into play, because the electron spin relaxation is decently influenced even by such small motions as librations.

In their series of works, Dzuba et.al. developed a potent approach to characterize the librations of nitroxide probes in molecular glasses.[S6,S7] In particular, the product $<\alpha^2>\tau_c$ can be experimentally obtained, where $<\alpha^2>$ is the mean square angular amplitude of motion and τ_c is the corresponding correlation time. This approach is based on the measurements of transverse relaxation times (T_2) of nitroxide in two definite spectral positions.

The theoretical consideration of spin relaxation induced by the fast (sub-microsecond) stochastic molecular librations predicts the exponential decay of the two-pulse electron spin echo (ESE) signal upon incrementing the time delay between two pulses. The decay rate is determined by spectral anisotropy at the position of the nitroxide spectrum (positions **I** and **II** in Fig.S1a). The nitroxide spectrum is split into three lines due to the hyperfine interaction (HFI) between the spin of unpaired electron and the spin of nitrogen nucleus (I=1). The central component (**I**) is influenced mainly by the anisotropy of the g-tensor, with the anisotropy of HFI being negligible; therefore, it possesses the smallest anisotropy and the narrowest linewidth. For the broadest high-field component (**II**), both the anisotropies influence the spectral shape in an additive way, so it is the most anisotropic and the broadest one. Therefore, the decay rates for the field positions (**I**) and (**II**) are essentially different. However, there are other additive relaxation mechanisms contributing to the resulting T_2 values. Therefore, in order to elucidate pure libration-induced relaxation, one should subtract the relaxation rates (inverse relaxation times T_2) in the two spectral positions (**I**) and (**II**), as is illustrated in Fig.S1a.

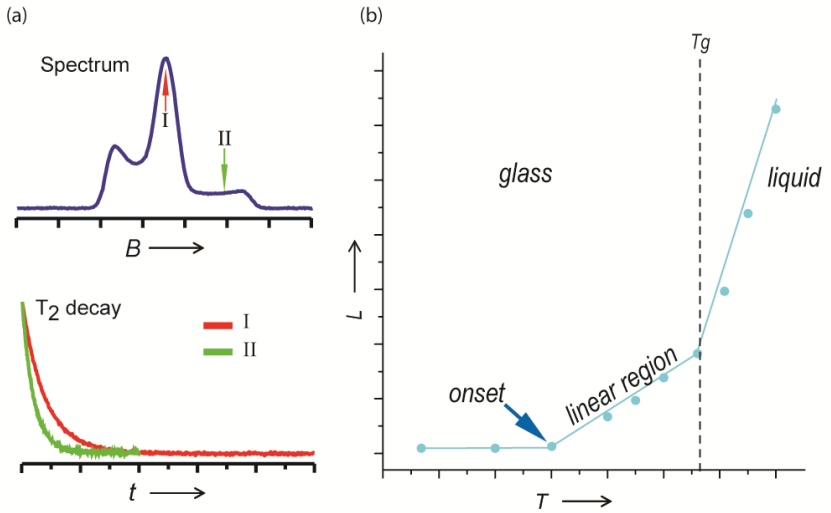

Figure S1. Sketch of the pulse EPR analysis scheme. (a) Two-pulse electron spin echo detected spectrum (top). The T_2 decay is measured by incrementing τ delay in $\pi/2$ - τ - π - echo sequence at two spectral positions **I** and **II**. Corresponding T_2 times are obtained by monoexponential analysis. (b) Typical $L(T)$ dependence showing low-temperature region of no librations, then their onset, linear region of effective librations, and, finally, transition into a liquid state with steep increase of molecular motion.

As a result, we obtain pure libration-based contribution, which we denoted $L \equiv (1/T_2^{II} - 1/T_2^{I})$. Redfield relaxation theory shows that for fast (sub-microsecond) and small-angle librations $L \approx C\langle\alpha^2\rangle\tau_c$, where $\langle\alpha^2\rangle$ and τ_c were defined above, and C is the numerical coefficient, whose value was semi-empirically determined to be $9 \cdot 10^{16}$ s^{-2} for nitroxide radicals.[S7]

However, not the absolute value of L at certain temperature, but the shape of the $L(T)$ dependence is most informative and has to be analyzed. Theory of atomic displacements predicts that $L(T)$ should linearly grow with temperature. Figure S1b sketches possible behaviors of $L(T)$ dependence. The onset of librations indicates the temperature where librations start to influence electron spin relaxation strong enough to be detected in ESE-based T_2 measurements. The slope of the $L(T)$ curve characterizes the intensity of librations. When glass softens and transforms into a liquid, the amplitude of the nitroxide motions drastically grows, leading to a steep rise of $L(T)$ until T_2 becomes too short to be measured. Thus, in general, no other behaviors are to be expected for the $L(T)$, unless some structural rearrangements occur. There is no reason for $L(T)$ curve to change from a rising trend to a decrease as T increases, because kT driving librations does grow. Thus, any deviations from monotonic linear growth indicate some structural changes in the glassy matrix surrounding the nitroxide.

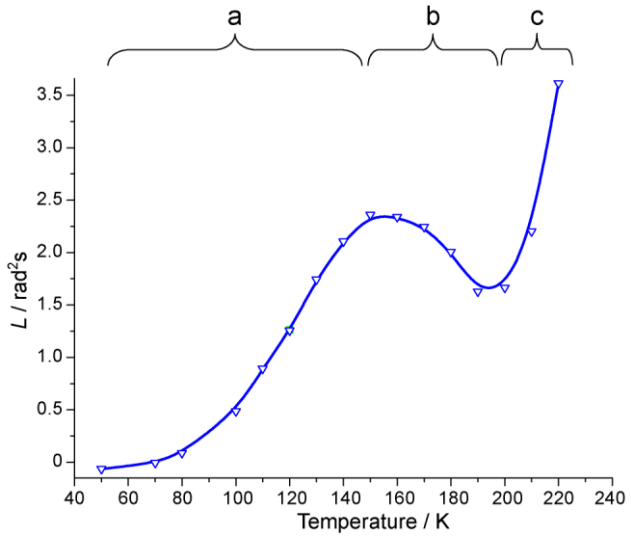

Figure S2. Representative schematic temperature dependence of the motional parameter L for nitroxide radical in ILs {a}, {b} and {c} indicate the motional regimes, see text for details. {b} is the region of anomaly.

However in the studied ILs $L(T)$ curve has three characteristic regions, that are marked as {a}, {b} and {c} in Figure S2. The rise of $L(T)$ function at ~70 K (region {a}) indicates the onset of stochastic molecular librations in IL. Further increase of the stochastic librations amplitude [growth of $L(T)$] is observed up to ~140 K (region {a} in Fig.S2). However, then the anomalous suppression of the stochastic librations is found within ~140−200 K (region {b}), which has never been observed in common organic glasses or biological membranes. At even higher temperatures T > 200 K, which are close to T_g of the studied ILs, the trend reverts to the rise again (region {c}), to be assigned to the unlocking of diffusive rotation of the radical in softened/melted IL. The linear growth of $L(T)$ in region {a} is a typical behavior, that was observed previously in various organic glasses and biological membranes. The nonlinear region {b} of $L(T)$ is the most interesting and represents the structural rearrangements in bulk IL. It was noticed that the position of local minimum of $L(T)$ curve clearly coincides with the T_g temperature of given IL.

VI. Arrangement of studied ILs according to the anion volume

Table S2 lists physical properties of studied ILs and arranges them according to the volume of anion V_{an}, which is important factor for confinement of ILs.

Table S2. Physical properties of studied ILs. T_m and T_g are the melting and glass transition points, V_{an} is the volume of anion taken from corresponding literature data (column "Reference").

Ionic liquid	T_m / K	T_g / K	V_{an} / Å^3	Reference
[Bmim]Cl	320	200	38.7	S8
[Bmim]Br	203	223	42.0	S9
			50	S8
[Bmim]BF_4	198	185	68.9	S9
			73	S10
			82.5	S8
[Bmim]PF_6	275	196	95.5	S9
			109	S10
[Bmim]CF_3SO_3	290	190	111.8	S9
			131	S10

References

S1 J. Dupont, C. S. Consorti, P. a. Z. Suarez and R. F. De Souza, Preparation of 1-butyl-3-methyl imidazolium-based room temperature ionic liquids, *Org. Synth.*, 2002, **79**, 236.

S2 I. A. Kirilyuk, Y. F. Polienko, O. A. Krumkacheva, R. K. Strizhakov, Y. V. Gatilov, I. A. Grigor'ev and E. G. Bagryanskaya, Synthesis of 2,5-bis(spirocyclohexane)-substituted nitroxides of pyrroline and pyrrolidine series, including thiol-specific spin label: An analogue of MTSSL with long relaxation time, *J. Org. Chem.*, 2012, **77**, 8016–8027.

S3 M. Y. Ivanov, S. A. Prikhod'ko, N. Y. Adonin, I. A. Kirilyuk, S. V. Adichtchev, N. V. Surovtsev, S. A. Dzuba and M. V. Fedin, Structural Anomalies in Ionic Liquids near the Glass Transition Revealed by Pulse EPR, *J. Phys. Chem. Lett.*, 2018, **9**, 4607–4612.

S4 S. Stoll and A. Schweiger, EasySpin, a comprehensive software package for spectral simulation and analysis in EPR, *J. Magn. Reson.*, 2006, **178**, 42–55.

S5 K. Kida, M. Okita, K. Fujita, S. Tanaka and Y. Miyake, Formation of high crystalline ZIF-8 in an aqueous solution, *CrystEngComm*, 2013, **15**, 1794.

S6 S. A. Dzuba, Libration motion of guest spin probe molecules in organic glasses: CW EPR and electron spin echo study, *Spectrochim. Acta - Part A Mol. Biomol. Spectrosc.*, 2000, **56**, 227–234.

S7 N. P. Isaev and S. A. Dzuba, Fast Stochastic Librations and Slow Rotations of Spin Labeled Stearic Acids in a Model Phospholipid Bilayer at Cryogenic Temperatures, *J. Phys. Chem. B*, 2008, **112**, 13285–13291.

S8 Y.Marcus, A simple empirical model describing the thermodynamics of hydration of ions of widely varying charges, sizes, and shapes, Biophys. Chem., 1994, **51**, 111-127.

S9 Y. V. Nelyubina, A. S. Shaplov, E. I. Lozinskaya, M. I. Buzin and Y. S. Vygodskii, A New Volume-Based Approach for Predicting Thermophysical Behavior of Ionic Liquids and Ionic Liquid Crystals, *J. Am. Chem. Soc.*, 2016, **138**, 10076–10079.

S10 I. Krossing, J.M. Slattery, C. Daguenet, P.J. Dyson, A. Oleinikova and H. Weingartner, Why are ionic liquids liquid? A simple explanation based on lattice and solvation energies, *J. Am. Chem. Soc.*, 2006, **128**, 13427–13434.